



Measurement of the Cross Section for W Boson + Photon Production at $\sqrt{s} = 1.96$ TeV

The DØ Collaboration
(Dated: March 20, 2004)

The cross section times branching ratio for events with both a W boson, which decays to an electron (muon) and a neutrino, and a photon has been measured at center-of-mass energy $\sqrt{s} = 1.96$ TeV. Data comprising 162 (82) pb^{-1} of $p\bar{p}$ collisions was obtained by the DØ Experiment in 2002 and 2003 in the electron (muon) decay channel. For a minimum photon transverse energy of 8 GeV and for a minimum lepton-photon separation $\Delta R > 0.7$, 146 (77) events were observed. These events include both those with a photon originating in the collision as well as those whose origin is radiation from the final state lepton. The combined result, representing the weighted average between the two channels, is $\sigma(p\bar{p} \rightarrow W\gamma + X \rightarrow \ell\nu\gamma + X) = 19.3 \pm 6.7(\text{stat.} + \text{sys.}) \pm 1.3(\text{lum.})$ pb, consistent with the Standard Model prediction.

Preliminary Results for Winter 2004 Conferences

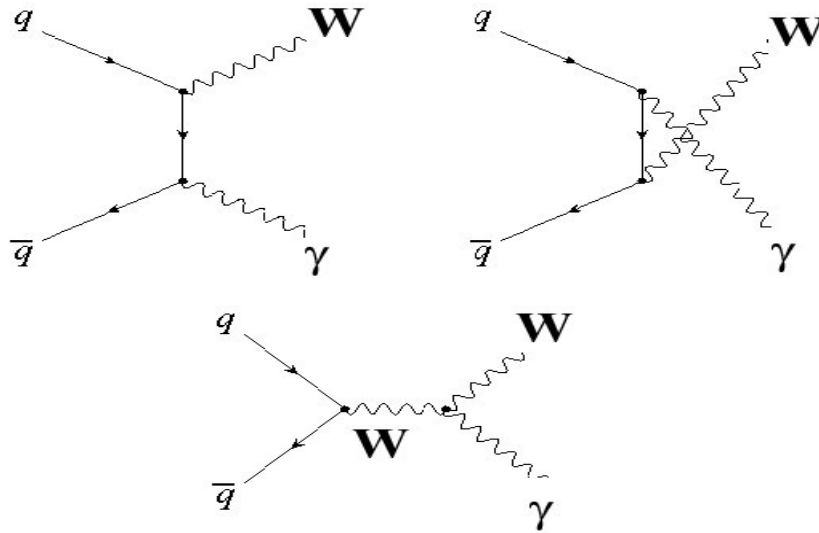


FIG. 1: The three tree-level diagrams for $W + \gamma$ production at the Tevatron. The lower diagram shown the trilinear gauge boson vertex.

I. INTRODUCTION

Interactions between gauge bosons, the W boson, Z boson and photon, are a consequence of the non-Abelian gauge symmetry of the Standard Model (SM). The gauge boson self-interactions are described by the trilinear gauge boson vertices and contribute to gauge boson pair production in $p\bar{p}$ collisions. The cross sections of these processes are relatively small, of order 1 to 100 pb at Tevatron energies, within the SM. The inclusion of non-SM (anomalous) couplings at the trilinear gauge boson vertices would enhance the production cross sections of gauge boson pairs, especially at large values of the gauge boson transverse momentum p_T , and at large values of the invariant mass of the gauge boson pair system [1]. Observation of anomalous gauge boson pair production would indicate physics beyond the SM.

A. $W + \gamma$ Production at the Tevatron

In proton-antiproton collisions the tree-level mechanisms for $W\gamma$ production are u - and t -channel diagrams with a pair of $q\bar{q}$ annihilations and the s -channel diagram, with the trilinear $WW\gamma$ vertex. These are shown in Fig. 1. An interesting feature of the Standard Model (SM) is that interference of amplitudes in s -channel diboson production with amplitudes in t - and u -channel production maintains unitarity in the $W\gamma$ cross section. In $W\gamma$ production this destructive interference results in a depletion in the distribution of rapidity difference $\Delta\eta$ between the photon and the decay lepton around $\Delta\eta = 0$ [2].

In events where the W boson has decayed leptonically, the signature is the high- E_T lepton, the missing transverse energy (\cancel{E}_T) due to the undetected neutrino, and a photon. This signature is shared by events with a W boson where the photon is the result of bremsstrahlung from the charged-lepton as shown in Fig. 2. In fact, the cross section for photon bremsstrahlung diverges as the separation between the photon and lepton and the energy of the photon is taken to zero. Therefore, we require a minimum photon E_T and minimum separation $\Delta R_{\ell\gamma}$, defined as $\sqrt{\Delta\eta^2 + \Delta\phi^2}$, between the photon and charged lepton.

In Run I, at $p\bar{p}$ center-of-mass energy 1800 GeV, we measured the cross section for $E_T(\gamma) > 10$ GeV and $\Delta R_{\ell\gamma} > 0.7$ as $11.3^{+1.7}_{-1.5} \pm 1.5$ pb. [3].

This analysis concentrates on the cross section for $p\bar{p} \rightarrow W\gamma + X$. It is a stepping-stone towards observation of detailed features in $W\gamma$ production and towards searches for new phenomena.

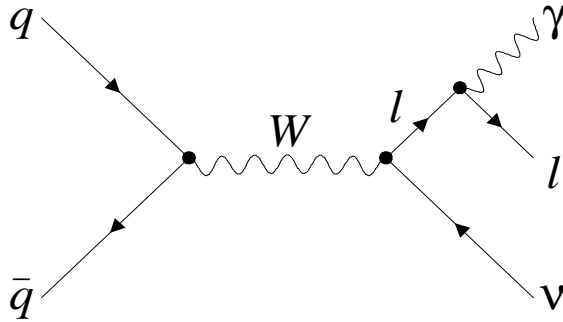


FIG. 2: The bremsstrahlung diagram for $W + \gamma$ production at the Tevatron. The photon has been radiated by the charged lepton.

II. DØ DETECTOR AND PARTICLE IDENTIFICATION

A. DØ Detector in “Run II”

The Run II DØ detector [4, 5] is comprised of the following main elements. A central-tracking system, which consists of a silicon microstrip tracker (SMT) and a scintillating-fiber tracker (CFT), both located within a 2 T superconducting solenoidal magnet. Central and forward preshower detectors located just outside of the superconducting coil (in front of the calorimetry) are constructed of three or four layers of extruded triangular scintillator strips. The next layer of detection involves three liquid-argon/uranium calorimeters: a central section (CC) covering $|\eta| < 1$, and two end calorimeters (EC) extending coverage to $|\eta| < 4.0$, all housed in separate cryostats [6]. In addition to the preshower detectors, scintillators between the CC and EC cryostats provide sampling of developing showers at $0.8 < |\eta| < 1.4$. The muon system resides beyond the calorimetry, and consists of a layer of tracking detectors and scintillation counters before 1.8 T toroids, followed by two more similar layers after the toroids. Tracking at $|\eta| < 1$ relies on 10 cm wide drift tubes [6], while 1 cm mini-drift tubes are used at $1 < |\eta| < 2$. Luminosity is measured using two sets of 24 scintillation counters, which are located between the CC and the two EC cryostats.

The trigger and data acquisition systems are designed to accommodate the large luminosity of Run II. Based on preliminary information from tracking, calorimetry, and muon systems, the output of the first level of the trigger reduces the beam crossing rate of 1.7 Mhz to ~ 1.8 kHz. At the next trigger stage, with more refined information, the rate is reduced further to 800 Hz. The third and final level of the trigger, with access to all the event information including precision readout, reduces the output rate to 50-60 Hz, which is written to tape.

B. Muon, Electron, and Photon Identification

Muons are identified by a high- p_T track in the muon spectrometer that matches spatially with a central track of $p_T > 20$ GeV/c. The muon is isolated if the E_T in a hollow cone of radius (0.4-0.1) in the calorimeter is less than 2.5 GeV. The muon trigger and identification efficiencies are determined by using events with at least one good muon and two high p_T tracks. These events are primarily Z boson decays. A typical single muon trigger has an efficiency of $58 \pm 3\%$. The muon identification efficiency is $58 \pm 4\%$.

Electrons and photons are first identified as an electromagnetic (EM) cluster found in the central or end calorimeters using a simple cone algorithm. The fraction of energy in the EM calorimeter within the cone is required to be greater than 0.9. Shower shape and isolation requirements distinguish the EM objects from hadronic jets.

Electrons are EM objects that have a track that coincides spatially and has E/p consistent with that of an electron.

The efficiency for electron ID is measured using Z boson decays. Photons are distinguished from electrons by the absence of a track in the inner trackers. The sum of p_T of tracks within a cone of size $\Delta R < 0.4$ is required to be less than 3 GeV/ c . The photon is required to be in the central calorimeter. Finally, the photons are required to have $E_T > 8$ GeV. The efficiency of the photon ID criteria is measured using a simultaneous fit to two data samples, one that contained $W\gamma \rightarrow \mu\nu\gamma$ candidates plus background events and a second that contained only background events. That efficiency is $47 \pm 13\%$ where the uncertainty is determined from the variation in the efficiency with changes in the procedure to discriminate photons from background. This is the dominant uncertainty in the analysis.

III. DATA SAMPLES AND CANDIDATE EVENT SELECTION

A. $W\gamma \rightarrow e\nu\gamma$ Candidate Selection

The candidate selection starts with a sample of 542873 events containing an EM object and \cancel{E}_T . This data sample is used for signal extraction and some background estimates. The candidate events are then required to satisfy at least one of several triggers that select events with a high- E_T EM object. The integrated luminosity yielded by those triggers totals 162.3 ± 10.5 pb $^{-1}$.

$W\gamma$ candidates are chosen by requiring the event to contain an electron that falls within the fiducial region of the calorimeter defined by $|\eta| < 1.1$ (CC) and $1.6 < |\eta| < 2.3$ (EC) and has $E_T > 25$ GeV, $\cancel{E}_T > 25$ GeV, and a photon with $E_T > 8$ GeV in the central calorimeter. The photons are required to be separated from the charged lepton such that $\Delta R_{\ell\gamma} > 0.7$. Finally, the transverse mass of the lepton and missing transverse energy, defined as $M_T = \sqrt{2E_T^{\text{lepton}}\cancel{E}_T(1 - \cos\Delta\phi)}$, where $\Delta\phi$ is the opening angle in the transverse plane between the charged lepton and the \cancel{E}_T , is required to be greater than 40 GeV/ c^2 .

A total of 146 events passed these selection criteria. Of these, 109 (37) had the electron in the CC (EC).

B. $W\gamma \rightarrow \mu\nu\gamma$ Candidate Selection

Events satisfying the evolving high- p_T single-muon trigger are gathered using three different muon triggers yielding a total luminosity of 82.0 ± 5.3 pb $^{-1}$. A subset of 15,276 events with objects satisfying loose muon and EM object criteria are preselected for further analysis.

To select the $W\gamma \rightarrow \mu\nu\gamma$ candidate events a number of criteria are applied that identify the W boson decay signature. An isolated muon was found in the muon system. The muon is required to be matched to a track in the inner tracker within the fiducial volume of full CFT coverage. The matched-track is required to have $p_T > 20$ GeV/ c . The event is rejected if any additional muon is present. The \cancel{E}_T in the event (compensated for the muon track) is required to be greater than 20 GeV.

The events thus selected are also required to have a photon with $E_T > 8$ GeV in the central calorimeter. The muon and the photon were required to be separated by $\Delta R > 0.7$.

A total of 77 events passed these selection criteria.

IV. GEOMETRIC AND KINEMATIC ACCEPTANCES

The geometric acceptance and the efficiency of the kinematic criteria are studied using an event generator [7, 8] referred-to as the ‘‘Baur Monte Carlo’’ and a parametrized simulation of the detector response (PMCS). This is a leading-order QCD Monte Carlo where the $W\gamma$ system is produced with no transverse momentum. To simulate the effects of higher-order QCD diagrams, mainly initial state gluon radiation, the $W\gamma$ system was given a transverse boost according to the distribution for $W\gamma$ events generated in Pythia [9] using CTEQ5L [10] parton distribution functions.

V. BACKGROUND ESTIMATES

The main backgrounds to $W\gamma$ is W +jets, where a jet is misidentified as a photon. The smaller backgrounds include: $Z\gamma$ where the \cancel{E}_T is due to an unreconstructed leptons or a mismeasured jet; $W\gamma \rightarrow \tau\nu\gamma$, where the τ has decay includes an electron or muon; and finally, any process which provides a lepton, an electron and missing E_T , due to

Background	Electron Channel (# events)	Muon Channel (# events)
W +jet	80.0 ± 7.4	$31. \pm 10.$
leX	3.7 ± 0.5	0.6 ± 0.6
$Z\gamma$	-	4.7 ± 2.0
$W\gamma \rightarrow \tau\nu\gamma$	3.4 ± 1.1	0.9 ± 0.3
Total	87.1 ± 7.5	$37. \pm 10.$

TABLE I: Backgrounds for the electron and muon channels.

inefficiencies in track reconstruction. These ‘leX’ backgrounds are treated inclusively as a single background. The backgrounds are summarized in Table V.

The W +jet background is estimated using the data samples. The probability P for a jet to be misidentified as a photon is measured using a large sample of events with multiple jets. It is found that P depends on the jet E_T and ranges from 0.0028 for jets with $E_T = 10$ GeV to 0.0010 for jets with $E_T = 50$ GeV. This probability is then folded with the number of jets in W +jet events in the two decay channels. The uncertainty in this background is driven by the uncertainty for a jet to be misreconstructed as a photon in the electron channel and by the difference in the background between two slightly different procedures in the muon channel. For the electron channel the W +jets background is 57.0 ± 5.5 (CC) and 23 ± 5 (EC) events. In the muon channel that background is 31 ± 10 events.

A variety of processes can cause the leX event topology (Drell-Yan, $t\bar{t}$, $Z \rightarrow \tau\tau$ etc.). To determine the leX background, events are selected with the same criteria as $W\gamma$ but requiring a track match to the ‘‘photon’’ object. The number of events passing this criteria provides an estimate of the background, i.e. the isolation requirement gives $N_{trackmatched} = N_{leX} \times \epsilon_T$, where $N_{trackmatched}$ is the number of such events, ϵ_T is the track finding efficiency and N_{leX} is the number of leX background events we wish to determine. Solving for N_{leX} the expected number of background is

$$N_{leX} = \frac{(1 - \epsilon_{TrkIso})}{\epsilon_T} \times N_{trackmatched}$$

where $1 - \epsilon_{TrkIso}$ is the inefficiency of the track isolation criterion for electrons. The background in the electron channel is $N_{eeX} = 3.0 \pm 0.5$ (CC) and 0.70 ± 0.20 (EC) events. In the muon channel $N_{\mu eX}$ is 0.6 ± 0.6 events.

To determine the $Z\gamma$ and $W\gamma \rightarrow \tau\nu\gamma$ backgrounds, events are generated using the Baur MC and then boosted using the Pythia derived distributions, as is done for the signal event generation. These events are then processed with the fast detector simulation (PMCS). The $Z\gamma$ and ‘‘ τ ’’ backgrounds are calculated as a fraction of the signal. The $Z\gamma$ backgrounds are 4.7 ± 2.0 events in the muon channel and insignificant in the electron channel. The ‘‘ τ ’’ backgrounds are 0.9 ± 0.3 events in the muon channel and 3.4 ± 1.1 events in the electron channel. Note that these backgrounds have ID efficiency uncertainties that are completely correlated with those expected for the signal.

VI. RESULTS

The full equation for the cross section times branching ratio is shown in Equation 1.

$$\sigma_{W\gamma \rightarrow \ell\nu\gamma} = \frac{(N - N_{bkg})}{\epsilon \times A \times L}, \quad (1)$$

where $\epsilon \times A$ is the total efficiency and acceptance of the cuts made on the reconstruction, trigger and kinematics of the charged lepton and photon, L is the integrated luminosity. The cross sections were calculated separately for the electron and muon channels. Table II summarizes the efficiencies, acceptances, and numbers of events used in the cross section calculations. Note that the muon channel is actually calculated separately in three data periods because of the evolution of the muon trigger and then combined. The results are $\sigma(W\gamma \rightarrow e\nu\gamma + X) = 17.8 \pm 3.6_{\text{stat.}} \pm 5.3_{\text{sys.}} \pm 1.1_{\text{lum.}}$ pb and $\sigma(W\gamma \rightarrow \mu\nu\gamma + X) = 22.0 \pm 4.2_{\text{stat.}} \pm 7.3_{\text{sys.}} \pm 1.4_{\text{lum.}}$ pb.

These were subsequently combined, taking the uncertainty in the photon efficiency and that in the luminosity as completely correlated, and the rest as uncorrelated. The result is $\sigma(W\gamma \rightarrow \ell\nu\gamma + X) = 19.3 \pm 4.2(\text{uncorrelated}) \pm 5.2(\text{correlated}) \pm 1.2(\text{lum.})$ pb. Combining the uncertainties gives $\sigma(p\bar{p} \rightarrow W\gamma + X \rightarrow \ell\nu\gamma + X) = 19.3 \pm 6.7(\text{stat.} + \text{sys.}) \pm 1.2(\text{lum.})$ pb.

The Standard Model prediction for the cross section is 16.4 ± 0.4 pb either decay channel. This comes from BAUR MC calculation using CTEQ5L PDFs. A K-factor of 1.33 is used to correct the cross section for processes not included in the leading order calculation. The uncertainty comes from the range of predictions using three different PDFs.

	Electron Channel	Muon Channel
Candidates	146 events	77 events
Acceptance \times Efficiency	0.0206 ± 0.0056	0.0226 ± 0.0063
Expected Signal + Background	142 ± 17	67 ± 13
Luminosity	162.3 ± 10.5 (pb)	82.0 ± 5.3

TABLE II: The number of candidates, the acceptance times efficiency, expected signal plus background, and the luminosity for the electron and muon channels.

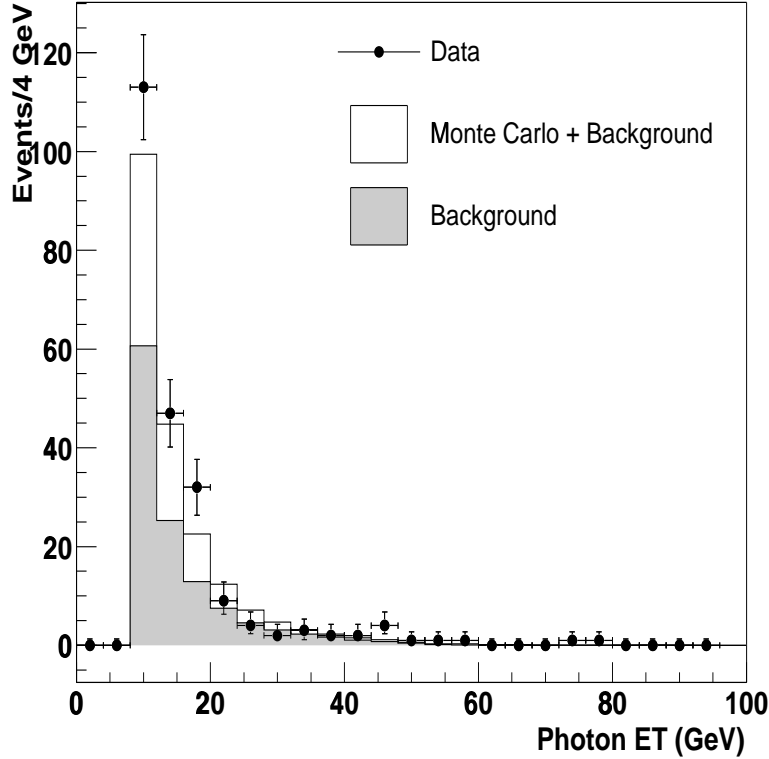


FIG. 3: The photon E_T spectrum for the combined samples. The candidate events are solid circles with uncertainties. The expected signal plus background is shown as unshaded histogram. The shaded histogram is the expected background only.

Figure 3 shows the combined photon E_T spectrum for the candidate events, the background, and the expected signal plus background. Figure 4 shows the separation ΔR between the charged-lepton and the photon. Figure 5 shows the transverse mass M_T of the charged-lepton and \cancel{E}_T . Figure 6 shows the 3-body transverse mass $M_{cluster}$ of the charged-lepton, photon, and \cancel{E}_T . This is defined as

$$M_T^2(l\gamma; \cancel{E}_T) = \left((M_{l\gamma}^2 + |\mathbf{p}_T(\gamma) + \mathbf{p}_T(l)|^2)^{\frac{1}{2}} + \cancel{E}_T \right)^2 - |\mathbf{p}_T(\gamma) + \mathbf{p}_T(l) + \cancel{E}_T|^2. \quad (2)$$

In events where the photon originated from bremsstrahlung, the 3-body transverse mass tends to be less than M_W . Whereas, in events that came from u -, t -, or s -channel production, the 3-body transverse mass tends to be greater than M_W .

VII. SUMMARY

The cross section times branching ratio for events with both a W boson and a photon has been measured at center-of-mass energy $\sqrt{s} = 1.96$ TeV. Data comprising 162 (82) pb^{-1} of $p\bar{p}$ collisions was obtained by the $D\mathcal{O}$ Experiment

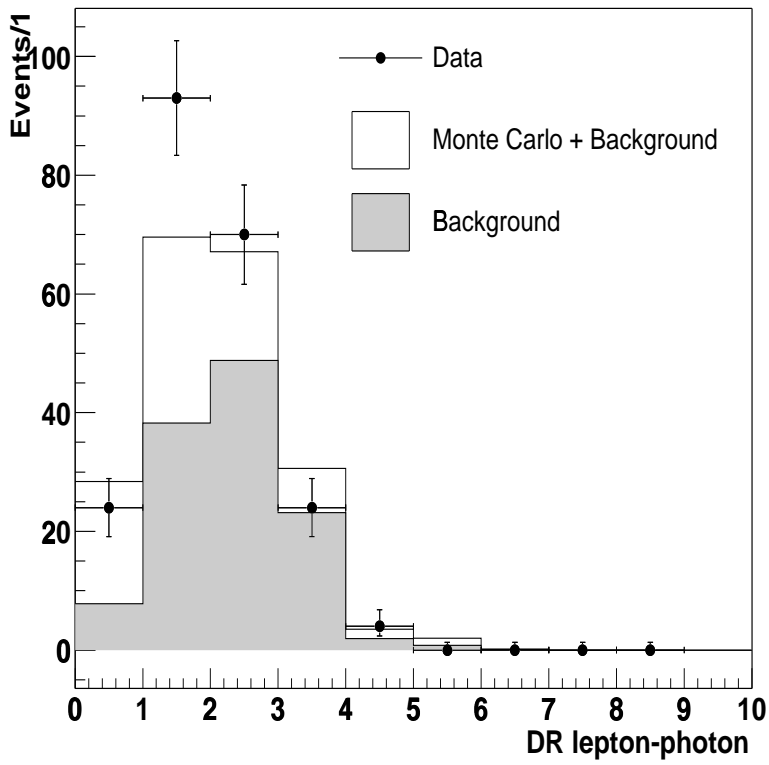


FIG. 4: The separation ΔR between the charged-lepton and the photon. The candidate events are solid circles with uncertainties. The expected signal plus background is shown as unshaded histogram. The shaded histogram is the expected background only.

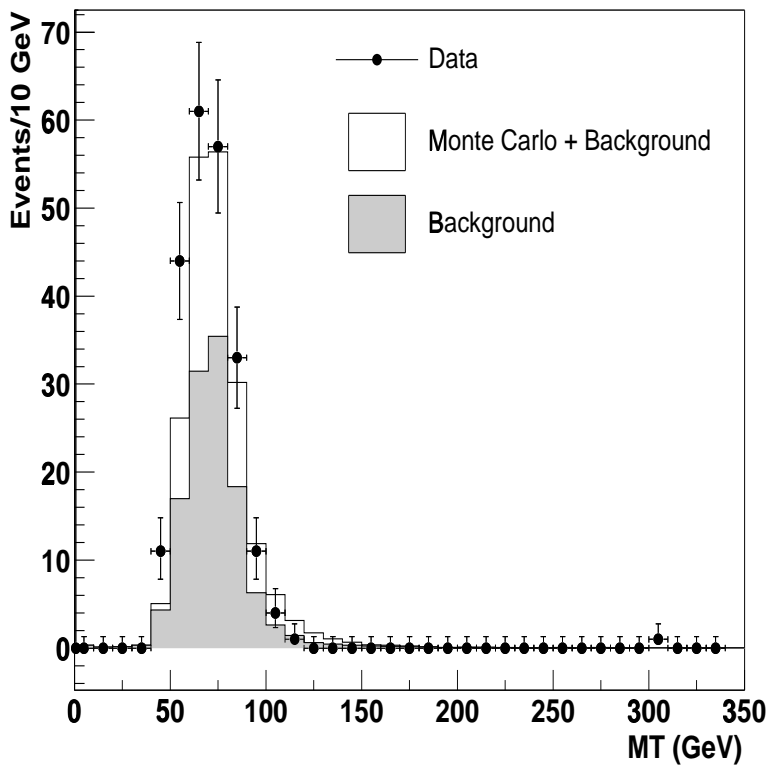


FIG. 5: The transverse mass M_T of the charged-lepton and \cancel{E}_T . The candidate events are solid circles with uncertainties. The expected signal plus background is shown as unshaded histogram. The shaded histogram is the expected background only.

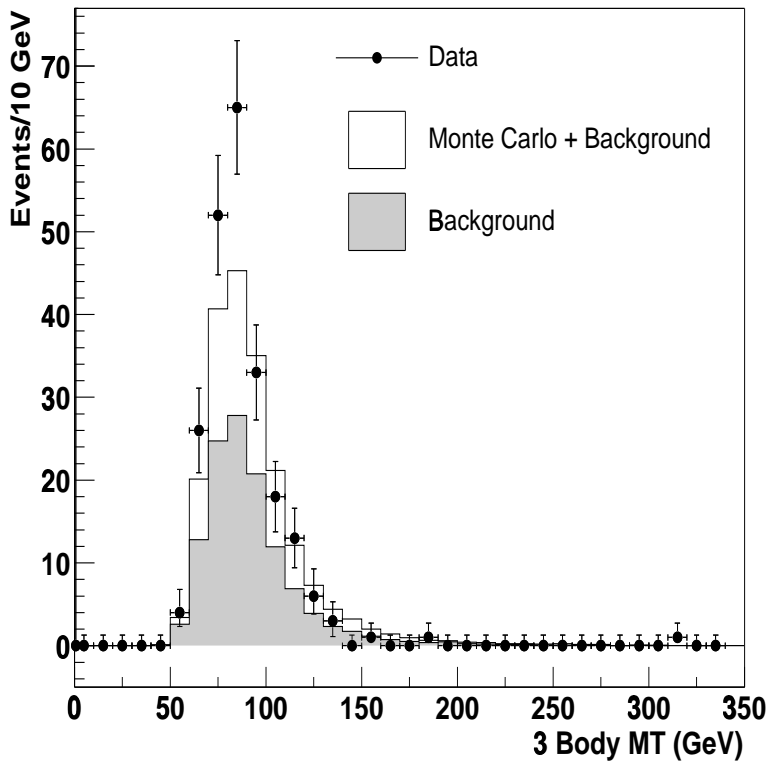


FIG. 6: The 3-body transverse mass M_T of the charged-lepton, photon, and \cancel{E}_T . The candidate events are solid circles with uncertainties. The expected signal plus background is shown as unshaded histogram. The shaded histogram is the expected background only.

in 2002 and 2003 in the electron (muon) decay channel. For a minimum photon transverse energy of 8 GeV and for a minimum lepton-photon separation $\Delta R > 0.7$, 146 (77) events were observed. These events include both those with a photon originating in the collision as well as those whose origin is radiation from the final state lepton. The combined result is $\sigma(p\bar{p} \rightarrow W\gamma + X \rightarrow \ell\nu\gamma + X) = 19.3 \pm 6.7(\text{stat.} + \text{sys.}) \pm 1.2(\text{lum.})$ pb, consistent with the Standard Model prediction.

Acknowledgments

We thank the staffs at Fermilab and collaborating institutions, and acknowledge support from the Department of Energy and National Science Foundation (USA), Commissariat à l’Energie Atomique and CNRS/Institut National de Physique Nucléaire et de Physique des Particules (France), Ministry for Science and Technology and Ministry for Atomic Energy (Russia), CAPES, CNPq and FAPERJ (Brazil), Departments of Atomic Energy and Science and Education (India), Colciencias (Colombia), CONACyT (Mexico), Ministry of Education and KOSEF (Korea), CONICET and UBACyT (Argentina), The Foundation for Fundamental Research on Matter (The Netherlands), PPARC (United Kingdom), Ministry of Education (Czech Republic), A.P. Sloan Foundation, Civilian Research and Development Foundation, Research Corporation, Texas Advanced Research Program, and the Alexander von Humboldt Foundation.

-
- [1] DØ Collaboration, B. Abbott *et al.*, “Studies of WW and WZ production and limits on anomalous $WW\gamma$ and WWZ couplings”, Phys. Rev. D **60**, 072002 (1999).
 - [2] U. Baur, S. Errede, and G. Landsberg, “Rapidity Correlations in $W\gamma$ Production at Hadron Colliders”, Phys. Rev. D **50**, 1917, (1994).
 - [3] DØ Collaboration, S. Abachi *et al.*, “Limits on Anomalous $WW\gamma$ Couplings from $p\bar{p} \rightarrow W\gamma + X$ Events at $\sqrt{s} = 1.8$ TeV”, Phys. Rev. Lett. **78**, 3634 (1997).
 - [4] T. LeCompte and H. T. Diehl, “The CDF and DØ Upgrades for Run II”, Annu. Rev. Nucl. Part. Sci. 50:71-117 (2000).

- [5] DØ Collaboration, V. Abazov *et al.*, “The DØ Detector for Run II”, in preparation.
- [6] DØ Collaboration, S. Abachi *et al.*, “The DØ Detector”, Nucl. Instrum. Methods A **338**, 185 (1994).
- [7] U. Baur and D. Zeppenfeld, “Probing the $WW\gamma$ Vertex at Future Hadron Colliders”, Nucl. Phys. **B308**, 127 (1988).
- [8] U. Baur and E. L. Berger, “Probing the $WW\gamma$ Vertex at the Tevatron Collider”, Phys. Rev. D **41**, 1476 (1990).
- [9] T. Sjöstrand, Comput. Phys. Commun. **82**, 74 (1994). We use Pythia version 6.202.
- [10] CTEQ Collaboration, H. L. Lai *et al.*, “Global QCD Analysis of Parton Structure of the Nucleon: CTEQ5 Parton Distributions”, Eur. Phys. J. C **12**, 375 (2000).